REFERENCES

Al-Shamrani, A.A., James, A., and Xiao, H. (2002) Destabilization of oil-water emulsions and separation by dissolved air flotation. Water Research, 36, 1503-1512.

Al-Shamrani, A.A., James, A., and Xiao, H. (2002) Separation of oil from water by dissolved air flotation. Colloids and Surfaces A: Physicochemical and Engineering Aspects, 209, 15-26.

Brandrup, J. and Immergut, E.H. (1989) Polymer Handbook 3rd ed. New York: John Wiley & Sons.

Carroll, B. (1996). The direct study of oily soil removal from solid substrates in detergency. Colloids and Surfaces A: Physicochemical and Engineering Aspects, 114, 161-164.

Chu, C.P., Lee, D.J., and Chang, C.Y. (2000) Thermogravimetric analysis of activated sludge flocculated with polyelectrolyte. Journal of Environmental Engineering, 126, 1082-1087

Coats, A.W. and Redfern, J.P. (1964) Kinetic parameters from Thermogravimetric data. Nature, 201, 68-69.

Drinan, J.E. (2001) Water and Wastewater Treatment: A Guide for the Nonengineering Professional. Lancester: Technomic Publshing.

Eckenfelder, W.W.Jr. (2000) Industrial Water Pollution Control 3rd ed. Boston: McGraw-Hill.

Gray, S.R., Harbour, P.J., and Dixon, D.R. (1997) Effect of polyelectrolyte charge density and molecular weight on the flotation of oil-in-water emulsions. Colloids and Surfaces A: Physicochemical and Engineering Aspects, 126, 85-95.

Holmberg, K., Jönsson, B., Kronberg, B., and Lindman, B. (2003) Surfactant and Polymer in Aqueous Solution 2nd ed. Chichester: John Wiley & Sons.

Dubdub, I.J.M. and Tiong, N.T. (2001) Recycling of plastic waste: Comprehensive kinetic pyrolysis study of PVC and PET polymers using TGA. Proceeding of 6th World Congress of Chemical Engineering, Melbourne.

Janiyani, K.L., Wate, S.R., and Soshi, S.R. (1993) Solubilization of hydrocarbons from oil sludge by synthetic surfactants. Journal of Chemical Technology and Biotechnology, 56, 305-308.

Kolev, V.L., Kochijashky, I.I., Danov, K.D., Kralchevsky, P.A., Broze, G., and Mehreteab A. (2003) Spontaneous detachment of oil drops from solid substrate: governing factor. Journal of Colloid and Interface Science, 257, 357-363.

Lange, K.R. (1994) Detergent and Cleaners. Munich: Hanser.

Lissant, K.J. (1983) Demulsification: Industrial Applications. New York: Marcel Dekker.

Liu, N., Fan, W., Dobachi, R., and Lin, Qizhao. (2000) New mass loss kinetic model for thermal decomposition of biomass. Chinease Science Bulletin, 45, 385-391

Lui, N.A., Fan, W., Dobashi, R., and Huang, L. (2002) Kinetic modeling of thermal decomposition of natural cellulosic in air atmosphere. Journal of Analytical and Applied Pyrolysis, 63, 303-325

Mabire, F., Audebert, R., and Quivoron, C. (1984) Journal of Colloid and Interface Science, 97, 120

Marinova, K.G., Alargova, R.G., Denkov, N.D., Velev, O.D., Petsev, D.N., Ivanov, I.B., and Borwankar, R.P. (1995) Charging of oil-water interfaces due to spontaneous adsorption of hydroxyl ions. Langmuir, 12, 2045-2051

Oudenhoven van, J.A.C.M., Cooper, G.R., Gricchi, G., Gineste, J., Pötal, R., Vissers, J., and Martin, D.E. (1995) Oil Refinery Waste Disposal Method, Quantity and Costs 1993 Survey.

Pinotti, A. and Zaritzky, N. (2001) Effect of aluminum sulfate and cationic polyelectrolytes on the destabilization of emulsified waste. Waste Management, 21, 535-542.

Punnarattanakun, P., Meeyoo, V., Rangsunvigit, P., Rirksomboon, T., Kitiyanan, B., and Kalambaheti, C. (2002) Pyrolysis of API separator sludge. Journal of Analytical and Applied Pyrolysis, 68-69, 547-560.

Riddick, T.M. (1964) Tappi, 47, 171A

Ríos, G., Pazos, J., and Coca, J. (1998) Destabilization of cutting oil emulsions using inorganic salts as coagulants. Colloids and surfaces A: Physicochemical and Engineering Aspects, 138, 383-389.

Rosen, M.J. (1988) Surfactant and Interfacial Phenomena 2nd ed. New York: John Wiley & Sons.

Rowe, A.W., Counce, R.M., Morton, S.A., Hu, M.Z.C., and Depaoli, D.W. (2002) Oil detachment from solid surface in aqueous surfactant solutions as a function of pH. Industrial Engineering Chemistry Research, 41, 1787-1795.

Schramm, L.L. (1992) Emulsions: fundamental and aplications in petroleum industry. Washington DC: American Chemical Society.

Stachusky, J. and Michalek, M. (1996) The effect of the ζ potential on the stability of a non-polar oil-in-water emulsion. Journal of Colloid and Interface Science, 184, 433-436.

Starkweather, B.K., Counce, R.M., and Zhang, X. (1999) Displacement of a hydrocarbon oil from a metal surface using a surfactant solution. Separation Science and Technology, 34(6-7), 1447-1462.

Thompson, L. (1994) The role of oil detachment mechanism in determining optimum detergency condition. Journal of Colloid and Interface Science, 163(1), 61-73.

Zouboulis, A.I. and Avranas, A. (2000) Treatment of oil-in-water emulsions by coagulation and dissolved air flotation. Colloids and surfaces A: Physicochemical and Engineering Aspects, 172, 153-161.

APPENDICES

Appendix A Optimum condition for the recovery of light components by using surfactant and electrolyte solution.

The optimum condition, i.e. sludge-to-surfactant ratio, stirring speed, stirring time and leaving time, was investigate prior to the further experiment. The studied parameter was varied while the other parameters would be kept constant. The results are shown in Figure A1-A4. The highest recovery was achieved at the sludge-to-surfactant ratio of 1: 8 after the mixture was stirred at 200 rpm for 30min. Moreover, the system required at least 12 for the complete oil phase separation. These conditions were used for the further experiments.

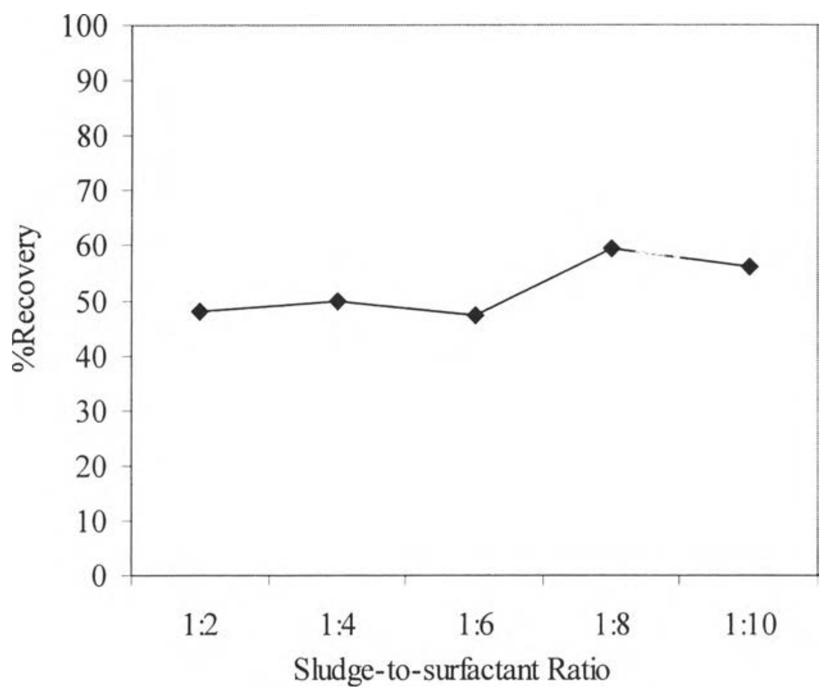

Figure A1 Recovery of light components at various sludge-to-surfactant ratios.

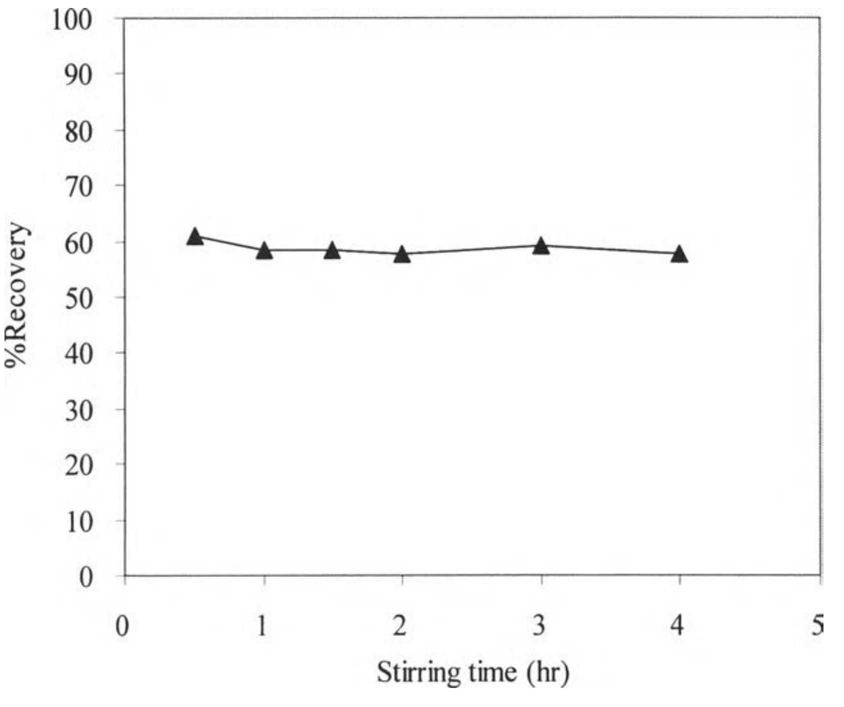

Figure A2 Recovery of light components at various stirring times.

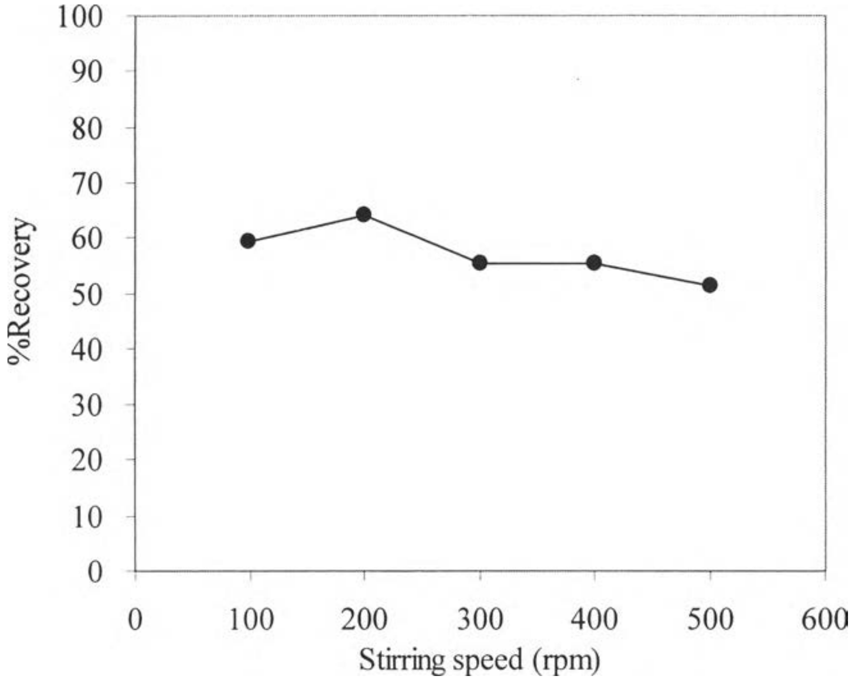

Figure A3 Recovery of light components at various stirring speeds.

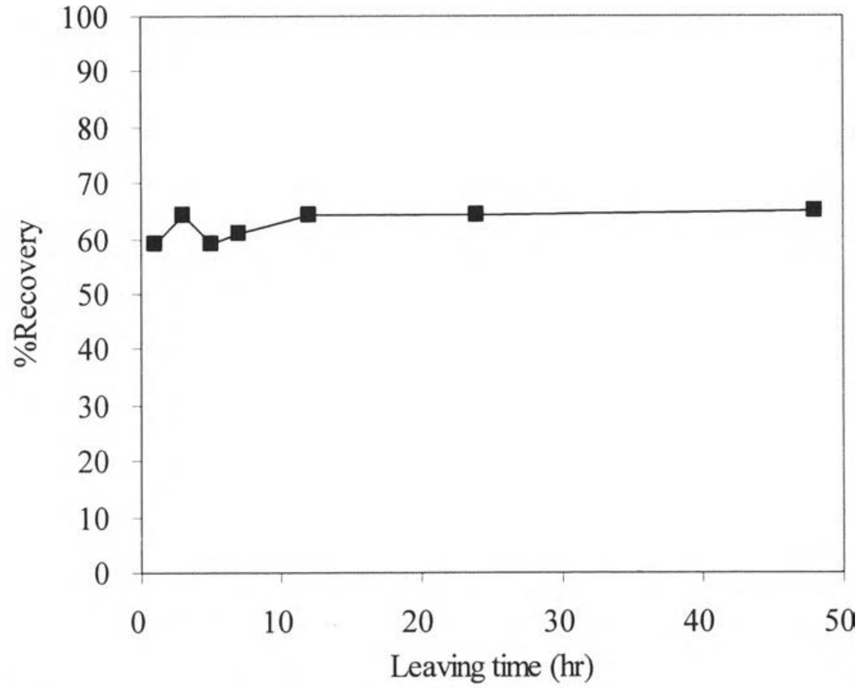

Figure A4 Recovery of light Components at various leaving times.

Appendix B Viscosity-average molecular weight of polyelectrolyte.

Table B1 The data of relative viscosity (η_{rel}), specific viscosity (η_{sp}), reduced viscosity (η_{red}) and inherent viscosity (η_{inh}) of Permafloc 2628

Concentration (g/100ml)	t (sec)	t_0 (sec)	η_{rel}	η_{sp}	η_{red}	η_{inh}
0.001	250.40	216.90	1.1545	0.1545	154.46	143.64
0.002	293.78	216.90	1.3544	0.3544	177.22	151.69
0.003	326.20	216.90	1.5039	0.5039	167.97	136.02
0.004	376.33	216.90	1.7351	0.7351	183.76	137.76

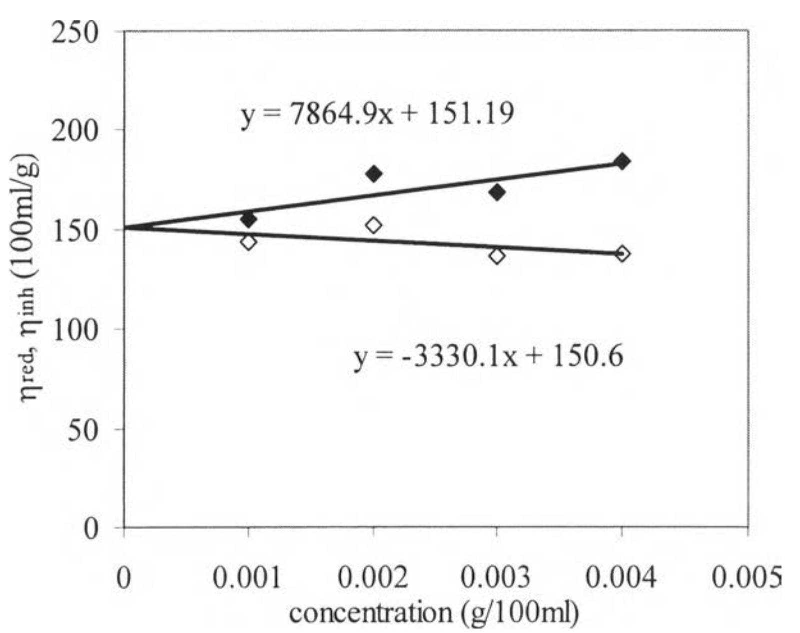

Figure B1 Plot of reduced viscosity (η_{red}) and inherent viscosity (η_{inh}) versus concentration of Permafloc 2628.

The intrinsic viscosity, [η], could be determined from y-intercept. The viscosity-average molecular weight of Permafloc 2628 was calculated base on Mark-Houwink equation.

$$[\eta] = KM^a$$

where [η] is intrinsic viscosity, M is viscosity-average molecular weight, K and a are constants. For polyacrylamind:

$K = 6.5 \times 10^{-3}$ ml/g

$a = 0.82$

y-intercept = 150.9

From calculation; $M = 5.80\times10^7$

The viscosity-average molecular weight of Permafloc 2628 obtained from the calculation was 5.80×10^7

Table B2 The data of relative viscosity (η_{rel}), specific viscosity (η_{sp}), reduced viscosity (η_{red}) and inherent viscosity (η_{inh}) of Permafloc 2525

Concentration (g/100ml)	t (sec)	t_0 (sec)	η_{rel}	η_{sp}	η_{red}	η_{inh}
0.001	249.44	216.90	1.1500	0.1500	150.01	139.77
0.002	282.81	216.90	1.3039	0.3039	151.91	132.68
0.003	319.82	216.90	1.4745	0.4745	158.17	129.44
0.004	353.89	216.90	1.6316	0.6316	157.89	122.39

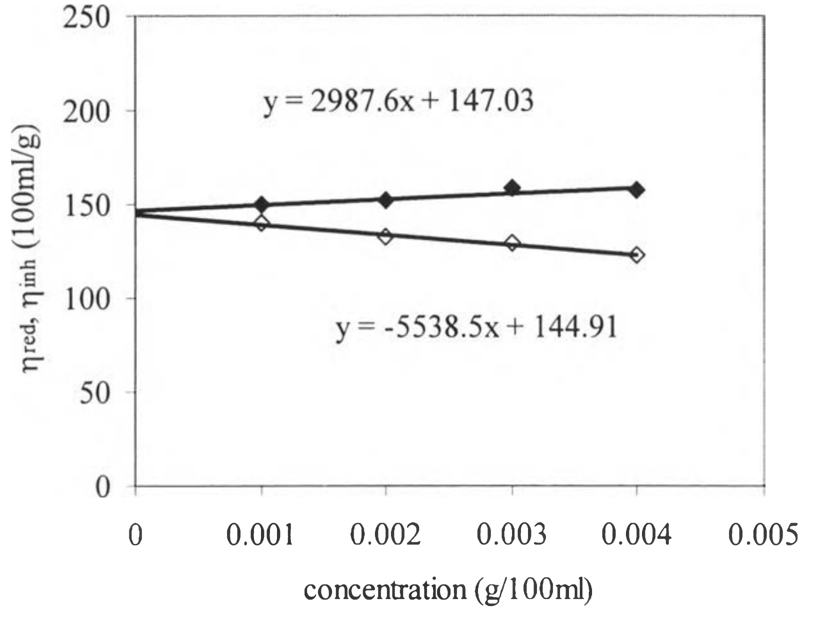

Figure B2 Plot of reduced viscosity (η_{red}) and inherent viscosity (η_{inh}) versus concentration of Permafloc 2525.

The intrinsic viscosity, $[\eta]$, could be determined from y-intercept. The viscosity-average molecular weight of Permafloc 2525 was calculated base on Mark-Houwink equation.

$$[\eta] = KM^{a}$$

where $[\eta]$ is intrinsic viscosity, M is viscosity-average molecular weight, K and a are constants. For polyacrylamind:

K = 6.5×10^{-3} ml/g

a = 0.82

y-intercept = 146.0

From calculation; M = 5.57×10^{7}

The viscosity-average molecular weight of Permafloc 2525 obtained from the calculation was 5.57×10^{7}

Table B3 The data of relative viscosity (η_{rel}), specific viscosity (η_{sp}), reduced viscosity (η_{red}) and inherent viscosity (η_{inh}) of Wachem Floctex 2602

Concentration (g/100ml)	t (sec)	t_0 (sec)	η_{rel}	η_{sp}	η_{red}	η_{inh}
0.001	249.88	216.90	1.1520	0.1520	152.04	141.53
0.002	290.29	216.90	1.3384	0.3384	169.18	145.72
0.003	330.04	216.90	1.5216	0.5216	173.88	139.93
0.004	368.42	216.90	1.6986	0.6986	174.64	132.44

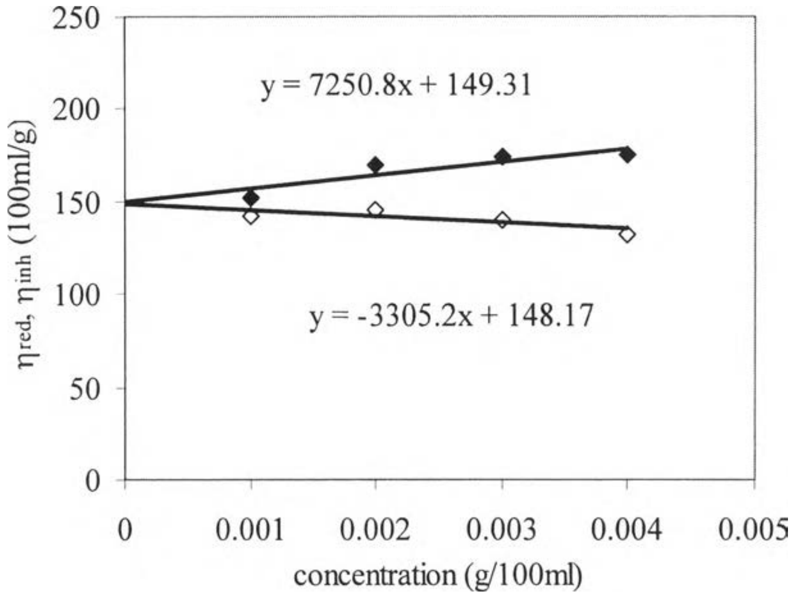

Figure B3 Plot of reduced viscosity (η_{red}) and inherent viscosity (η_{inh}) versus concentration of Wachem Floctex 2602.

The intrinsic viscosity, $[\eta]$, could be determined from y-intercept. The viscosity-average molecular weight of Wachem Floctex 2602 was calculated base on Mark-Houwink equation.

$$[\eta] = KM^{a}$$

where [η] is intrinsic viscosity, M is viscosity-average molecular weight, K and a are constants. For polyacrylamind:

K = 6.5×10^{-3} ml/g

a = 0.82

y-intercept = 148.7

From calculation; M = 5.70×10^{7}

The viscosity-average molecular weight of Wachem Floctex 2602 obtained from the calculation was 5.70×10^{7}

Table B4 The data of relative viscosity (η_{rel}), specific viscosity (η_{sp}), reduced viscosity (η_{red}) and inherent viscosity (η_{inh}) of Wachem Floctex 2431

Concentration (g/100ml)	t (sec)	t_0 (sec)	η_{rel}	η_{sp}	η_{red}	η_{inh}
0.001	246.45	216.90	1.1362	0.1362	136.22	127.71
0.002	286.44	216.90	1.3206	0.3206	160.30	139.05
0.003	321.65	216.90	1.4829	0.4829	160.98	131.34
0.004	361.08	216.90	1.6647	0.6647	166.18	127.41

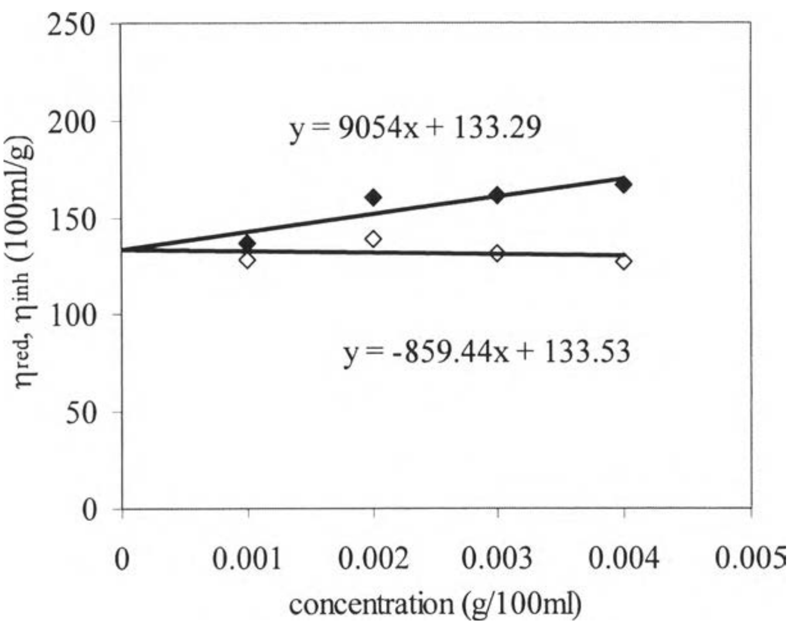

Figure B4 Plot of reduced viscosity (η_{red}) and inherent viscosity (η_{inh}) versus concentration of Wachem Floctex 2431.

The intrinsic viscosity, [η], could be determined from y-intercept. The viscosity-average molecular weight of Wachem Floctex 2431 was calculated base on Mark-Houwink equation.

$$[\eta] = KM^a$$

where [η] is intrinsic viscosity, M is viscosity-average molecular weight, K and a are constants. For polyacrylamind:

K = 6.5×10^{-3} ml/g

a = 0.82

y-intercept = 133.4

From calculation; M = 4.99×10^7

The viscosity-average molecular weight of Wachem Floctex 2431 obtained from the calculation was 4.99×10^7

Table B5 The data of relative viscosity (η_{rel}), specific viscosity (η_{sp}), reduced viscosity (η_{red}) and inherent viscosity (η_{inh}) of Wachem Floctex 2413

Concentration (g/100ml)	t (sec)	t_0 (sec)	η_{rel}	η_{sp}	η_{red}	η_{inh}
0.001	244.78	216.90	1.1286	0.1286	128.55	120.94
0.002	280.51	216.90	1.2933	0.2933	146.63	128.59
0.003	312.14	216.90	1.4391	0.4391	146.36	121.33
0.004	340.09	216.90	1.5680	0.5680	141.99	112.45

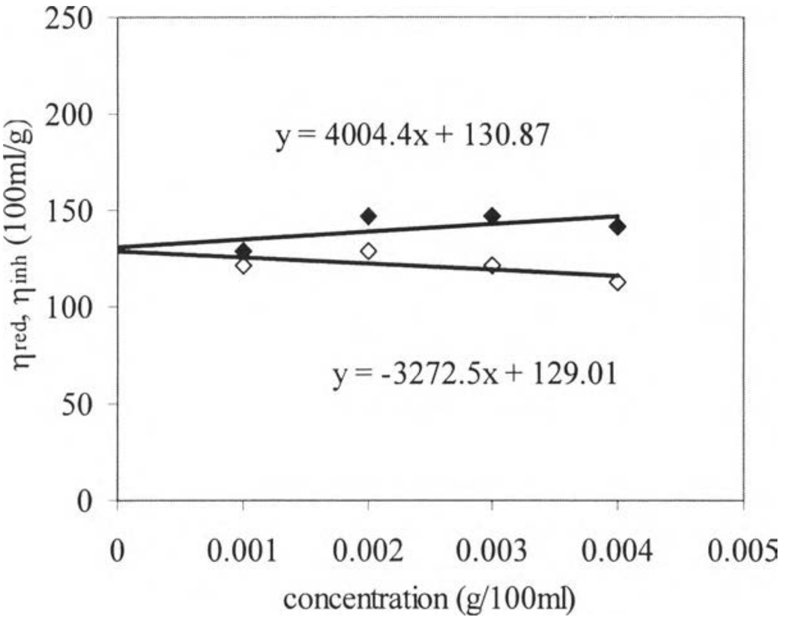

Figure B5 Plot of reduced viscosity (η_{red}) and inherent viscosity (η_{inh}) versus concentration of Wachem Floctex 2413.

The intrinsic viscosity, $[\eta]$, could be determined from y-intercept. The viscosity-average molecular weight of Wachem Floctex 2413 was calculated base on Mark-Houwink equation.

$$[\eta] = KM^a$$

where [η] is intrinsic viscosity, M is viscosity-average molecular weight, K and a are constants. For polyacrylamind:

K = 6.5×10^{-3} ml/g

a = 0.82

y-intercept = 129.9

From calculation; M = 4.83×10^{7}

The viscosity-average molecular weight of Wachem Floctex 2413 obtained from the calculation was 4.83×10^{7}

Appendix C Mathematic modeling

The thermal decomposition of the sludge can be expressed by

$$\ln\left(\frac{F(x)}{T^2}\right) = \ln\frac{A_i R}{\beta E_{ai}}\left(1 - \frac{2RT}{E_{ai}}\right) - \frac{E_{ai}}{RT},$$

where

$$F(x) = \begin{cases} -\ln(1-x) & n = 1 \\ \dfrac{1-(1-x)^{1-n}}{1-n} & n \neq 1 \end{cases}.$$

The independent pseudo bi-component model is applied for the weight loss of the sludge.

$$\frac{dx}{dT} = \begin{cases} \dfrac{dx_1}{dT} & W_{10} < W < W_{1\infty} \\ \dfrac{dx_2}{dT} & W_{1\infty} = W_{20} < W < W_{2\infty} \end{cases}.$$

The DTG data were divided into two temperature intervals. A plot of $\ln\left(\frac{F(x)}{T^2}\right)$ against $\frac{1}{T}$ should result in a straight line of the slope $\frac{-E_{ai}}{R}$ and the y-intercept $\ln\frac{A_i R}{\beta E_{ai}}\left(1 - \frac{2RT}{E_{ai}}\right)$ for the correct reaction order as shown in Figure C1-C12. Activation energy (E_{ai}) and pre-exponential factor (A_i) of each section can be calculated from the slope and y-intercept, respectively.

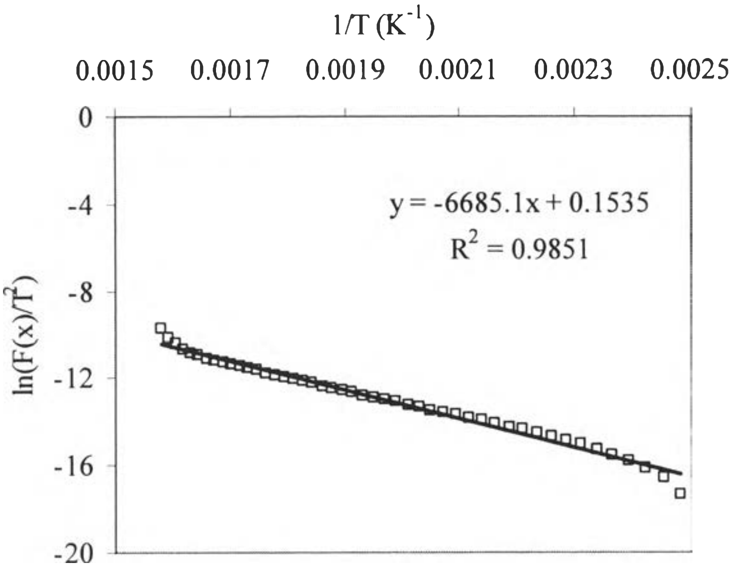

Figure C1 Relationship between $\ln\left(\frac{F(x)}{T^2}\right)$ and $\frac{1}{T}$ with equation and R^2, n = 1.6, of first reaction zone of original sludge pyrolysis (120-365°C) for 5°C/min heating rate.

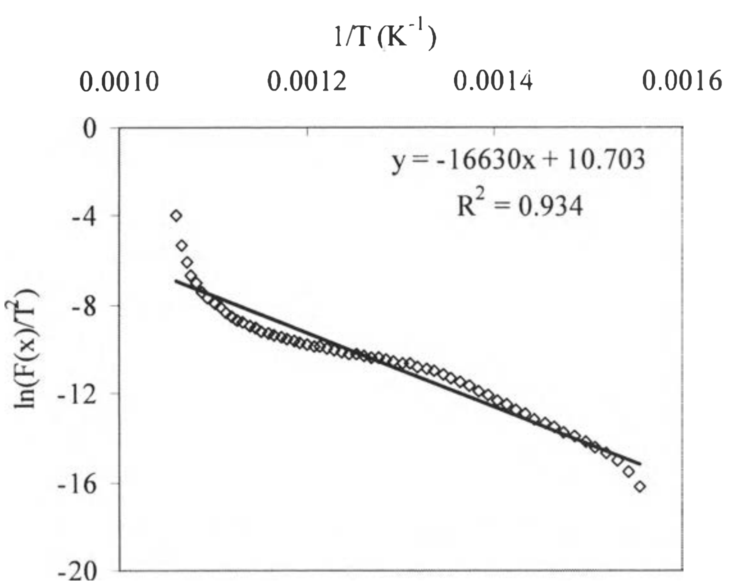

Figure C2 Relationship between $\ln\left(\frac{F(x)}{T^2}\right)$ and $\frac{1}{T}$ with equation and R^2, n = 3.0, of second reaction zone of original sludge pyrolysis (365-680°C) for 5°C/min heating rate.

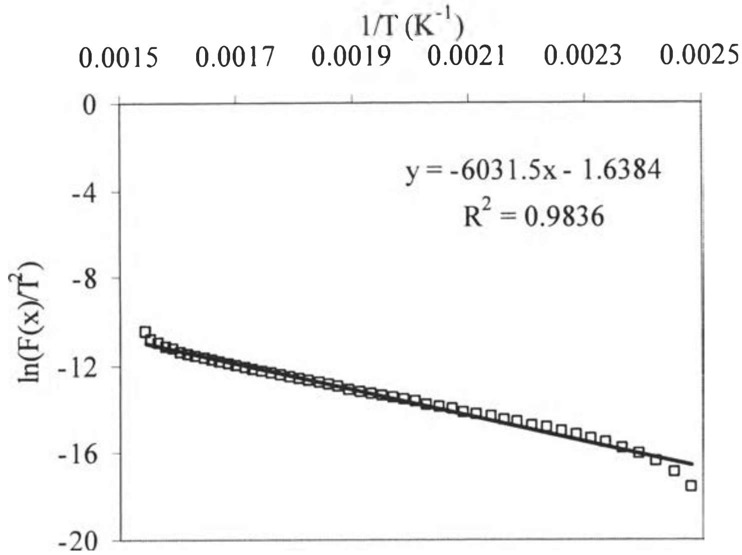

Figure C3 Relationship between $\ln\left(\frac{F(x)}{T^2}\right)$ and $\frac{1}{T}$ with equation and R^2, n = 1.4, of first reaction zone of original sludge pyrolysis (120-380°C) for 10°C/min heating rate.

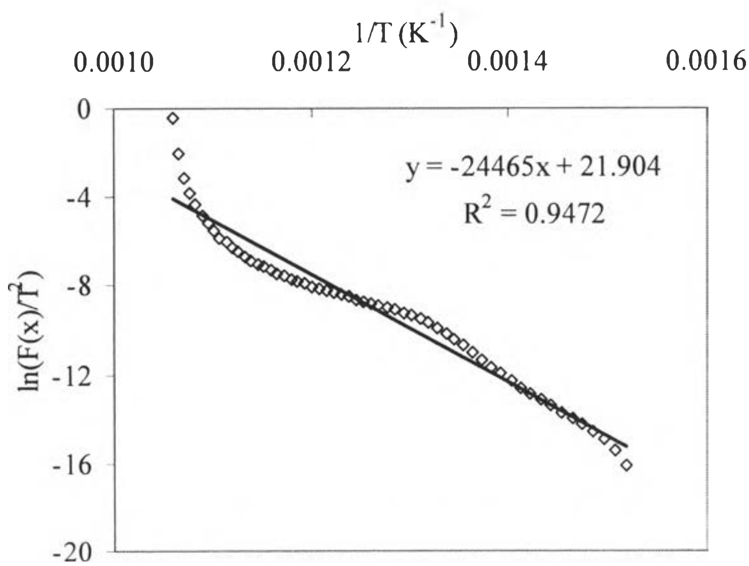

Figure C4 Relationship between $\ln\left(\frac{F(x)}{T^2}\right)$ and $\frac{1}{T}$ with equation and R^2, n = 3.6, of second reaction zone of original sludge pyrolysis (380-680°C) for 10°C/min heating rate.

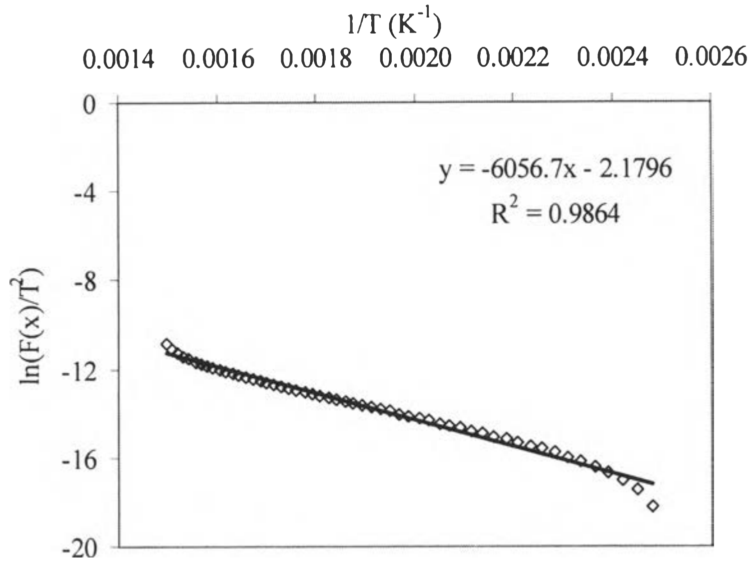

Figure C5 Relationship between $\ln\left(\frac{F(x)}{T^2}\right)$ and $\frac{1}{T}$ with equation and R^2, n = 1.3, of first reaction zone of original sludge pyrolysis (120-400°C) for 20°C/min heating rate.

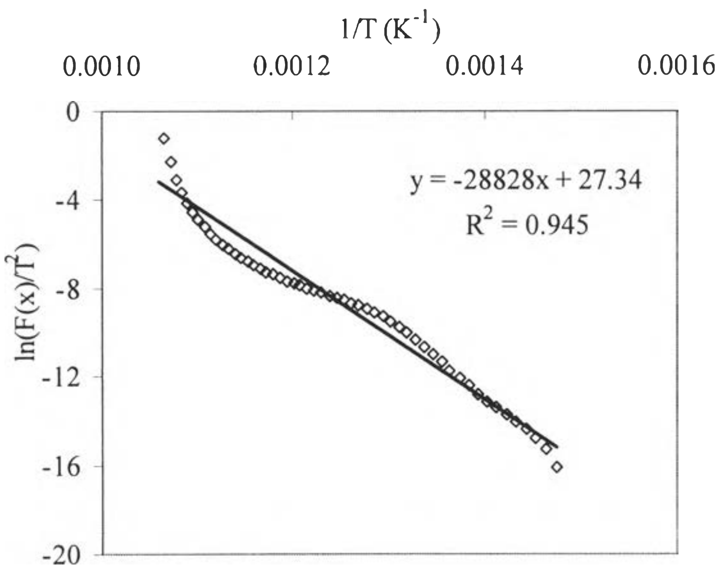

Figure C6 Relationship between $\ln\left(\frac{F(x)}{T^2}\right)$ and $\frac{1}{T}$ with equation and R^2, n = 3.8, of second reaction zone of original sludge pyrolysis (400-680°C) for 20°C/min heating rate.

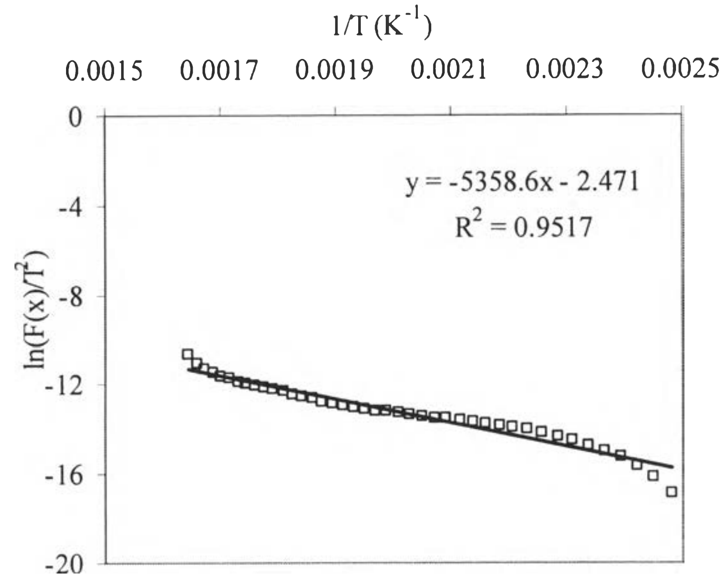

Figure C7 Relationship between $\ln\left(\frac{F(x)}{T^2}\right)$ and $\frac{1}{T}$ with equation and R^2, n = 1.4, of first reaction zone of treated sludge pyrolysis (120-340°C) for 5°C/min heating rate.

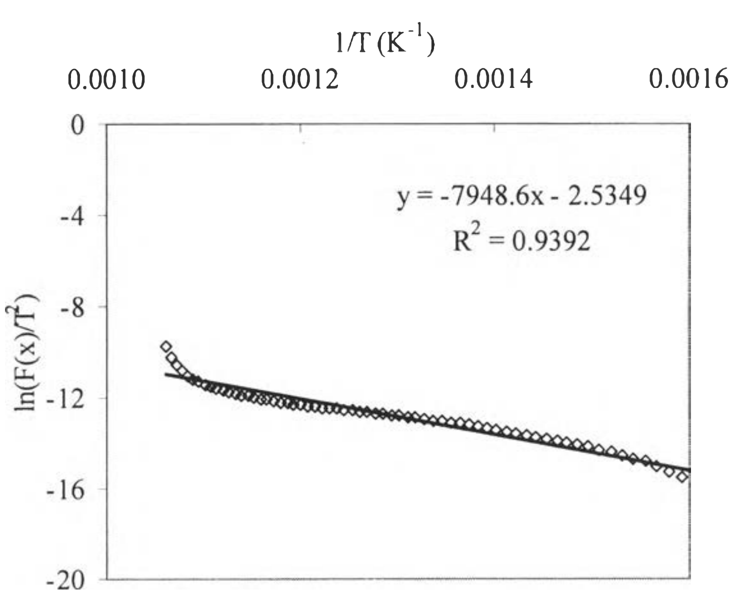

Figure C8 Relationship between $\ln\left(\frac{F(x)}{T^2}\right)$ and $\frac{1}{T}$ with equation and R^2, n = 1.8, of second reaction zone of treated sludge pyrolysis (340-680°C) for 5°C/min heating rate.

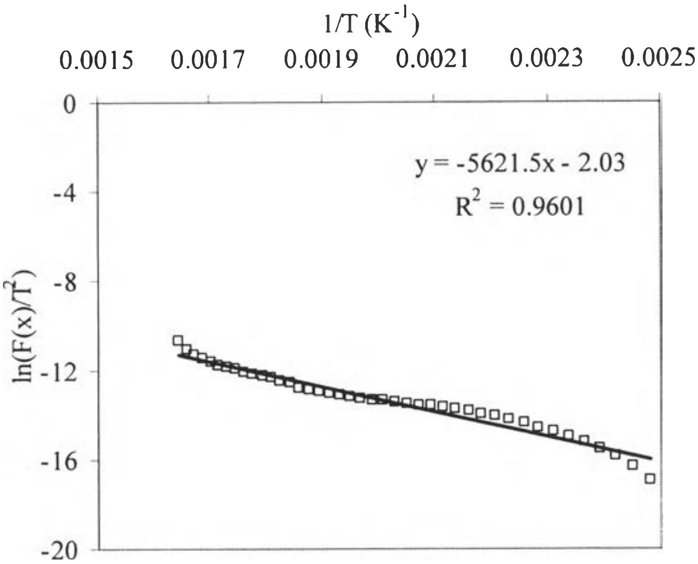

Figure C9 Relationship between $\ln\left(\frac{F(x)}{T^2}\right)$ and $\frac{1}{T}$ with equation and R^2, n = 1.4, of first reaction zone of treated sludge pyrolysis (120-340°C) for 10°C/min heating rate.

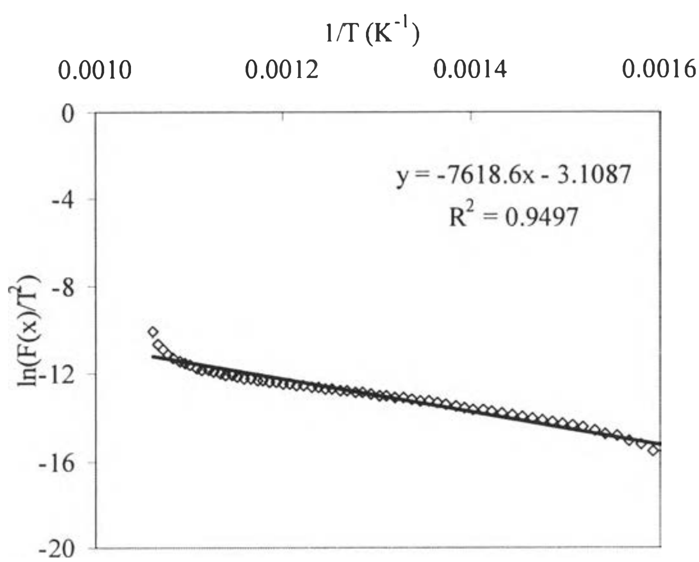

Figure C10 Relationship between $\ln\left(\frac{F(x)}{T^2}\right)$ and $\frac{1}{T}$ with equation and R^2, n = 1.7, of second reaction zone of treated sludge pyrolysis (340-680°C) for 10°C/min heating rate.

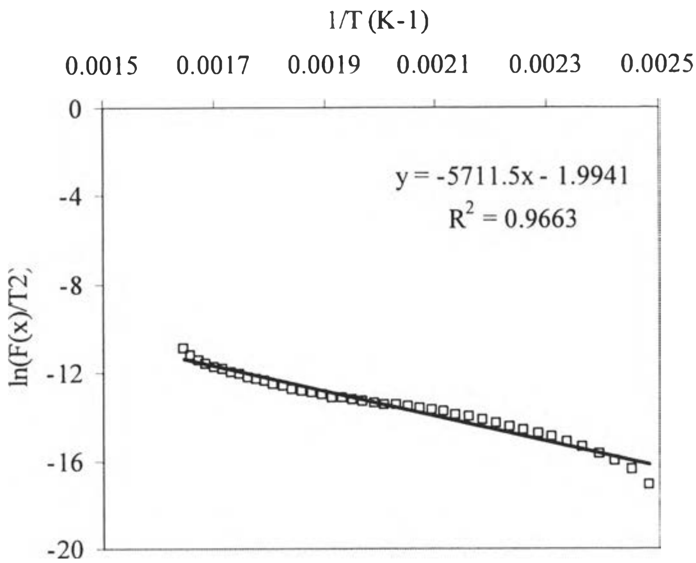

Figure C11 Relationship between $\ln\left(\frac{F(x)}{T^2}\right)$ and $\frac{1}{T}$ with equation and R^2, n = 1.3, of first reaction zone of treated sludge pyrolysis (120-340°C) for 20°C/min heating rate.

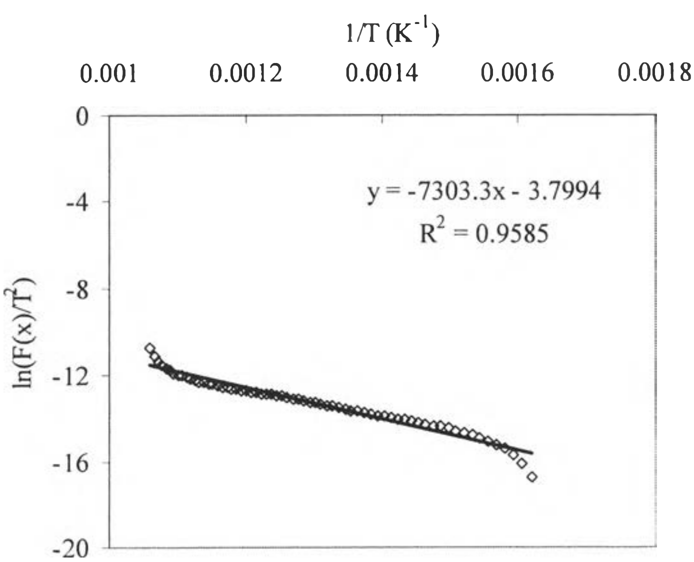

Figure C12 Relationship between $\ln\left(\frac{F(x)}{T^2}\right)$ and $\frac{1}{T}$ with equation and R^2, n = 1.5, of second reaction zone of treated sludge pyrolysis (340-680°C) for 20°C/min heating rate.

The pre-exponential factor (A_i) of each section can be calculated from

$$y - \text{intercept} = \frac{A_{iR}}{\beta E_{ai}}\left(1 - \frac{2RT}{E_{ai}}\right)$$

Then, the values of A_i at various temperature are plotted to express the relationship between A_i and T. The relationship between A_i and T are shown in Table C1.

Table C1 The relationship between pre-exponential factor (A) and temperature (T)

Type of sludge	Heating rate (°C/min)	Reaction step	Relation function	Temperature range (K)
Original sludge	5	1	$A(T) = 0.3219T^2+575.29T+2\times10^6$	120-365
		2	$A(T) = 4019.8T^2+2\times10^7T+2\times10^{11}$	365-680
	10	1	$A(T) = 0.0649T^2+93.308T+334664$	120-380
		2	$A(T) = 2\times10^8T^2+2\times10^{12}T+2\times10^{16}$	380-680
	20	1	$A(T) = 0.0394T^2+55.848T+202610$	120-400
		2	$A(T) = 4\times10^{10}T^2+4\times10^{14}T+6\times10^{18}$	400-680
Treated sludge	5	1	$A(T) = 0.0329T^2+38.212T+127428$	120-340
		2	$A(T) = 0.0214T^2+34.924T+177664$	340-680
	10	1	$A(T) = 0.048T^2+62.097T+211095$	120-340
		2	$A(T) = 0.0132T^2+19.395T+97900$	340-680
	20	1	$A(T) = 0.0302T^2+67.171T+230037$	120-340
		2	$A(T) = 0.0074T^2+9.6915T+48841$	340-680

Refined A_i can be obtained from

$$A_i = \frac{\int_{T_0}^{T} Ai(T)dT}{dT}$$

The values of pre-exponential are shown in Table C2.

Table C2 Pre-exponential factor of each temperature range

Type of sludge	Heating rate (°C/min)	Reaction step	A (min^{-1})	Temperature range (K)
Original sludge	5	1	2.39×10^{6}	120-365
		2	2.18×10^{11}	365-680
	10	1	4.02×10^{5}	120-380
		2	2.17×10^{16}	380-680
	20	1	2.44×10^{5}	120-400
		2	6.35×10^{18}	400-680
Treated sludge	5	1	1.55×10^{5}	120-340
		2	2.18×10^{5}	340-680
	10	1	2.55×10^{5}	120-340
		2	1.21×10^{5}	340-680
	20	1	2.77×10^{5}	120-340
		2	6.10×10^{4}	340-680

In order to obtain the refined E_{ai}, the values activation energy for each temperature were calculated.

$$f(E_{ai}) = \ln\left(\frac{F(x)}{T^2}\right) - \ln\frac{A_i R}{\beta E_{ai}}\left(1-\frac{2RT}{E_{ai}}\right)+\frac{E_{ai}}{RT}=0$$

Numerical method is used to solve this equation. The values activation energy are shown in Table C3.

Table C3 Activation energy of each temperature range

Type of sludge	Heating rate (°C/min)	Reaction step	E_a (kJ/mol)	Temperature range (K)
Original sludge	5	1	55.58	120-365
		2	138.25	365-680
	10	1	50.15	120-380
		2	203.39	380-680
	20	1	50.36	120-400
		2	239.67	400-680
Treated sludge	5	1	44.55	120-340
		2	66.09	340-680
	10	1	46.74	120-340
		2	63.34	340-680
	20	1	47.49	120-340
		2	60.72	340-680

CURRICULUM VITAE

Name: Ms. Kraumas Supaphol

Date of Birth: October 21, 1979

Nationality: Thai

University Education:

1998-2002 Bachelor degree of Science in Chemical Technology (2nd class honor), Faculty of Science, Chulalongkorn University

Proceeding:

Supaphol, K., Rangsunvigit, P., Meeyoo, V., Rirksomboon, T., Kitiyanan, B., and Kalambaheti, C. (2003). Recovery of Light Components from API Separator Sludge. Annual Conference of Thai Institute of Chemical Engineering and Applied Chemistry (TIChE), 30-31st October, Nakornnayok, Thailand.